https://doi.org/10.5194/egusphere-2024-657
Preprint. Discussion started: 19 March 2024

Investigating the responses of sun-induced chlorophyll fluorescence, gross primary production and their inter-relationship to abiotic factors changes in a temperate deciduous forest

Hamadou Balde[1,2,3,4], Gabriel Hmimina[1], Yves Goulas[1], Gwendal Latouche[2], Abderrahmane Ounis[1], Daniel Berveiller[2], Kamel Soudani[2]

[1]Laboratoire de Météorologie Dynamique, Sorbonne Université, IPSL, CNRS/L'École polytechnique, 91128, Palaiseau Cedex, France

[2]Ecologie Systématique et Evolution, Université Paris-Saclay, CNRS, AgroParisTech, 91190, Gif-sur-Yvette, France

[3]Centre national d'études spatiales (CNES), 18 av. Edouard Belin, 31400 Toulouse

[4]ACRI-ST, 260 Route du Pin Montard, BP 234, 06904 Sophia-Antipolis, France

Correspondence to: Hamadou Balde (hamadousalimatou@gmail.com)

Abstract. Far-red Sun-Induced chlorophyll Fluorescence (SIF) is increasingly used as a proxy of vegetation Gross Primary Production (GPP) across different ecosystems and at spatiotemporal resolutions going from proximal to satellite-based remote sensing measurements. However, the use of SIF to probe variations in GPP in forests is challenged by (1) confounding factors such as canopy structure and sun-canopy geometry, and by (2) leaf physiological and biochemical properties along with abiotic factors (light intensity, temperature, soil water content, atmospheric vapour pressure deficit, etc.) that can influence SIF and GPP in a different way. To provide insights into understanding the complex drivers of GPP and SIF variations and of their relationships, we examined how SIF and GPP changed at daily and seasonal scales and how canopy structure and environmental conditions affected SIF and GPP relationships in a deciduous oak forest. To do so, we combined canopy scale SIF measurements, spectral vegetation indices, environmental variables measurements, including diffuse and direct radiations in the spectral range of the Photosynthetically Active Radiation (PAR), air and canopy temperature, soil water content (SWC), atmospheric Vapour Pressure Deficit (VPD), and GPP estimated from eddy covariance measurements. Canopy chlorophyll fluorescence was also measured using an active system with an artificial light source, referred to as LIF (LED Induced chlorophyll Fluorescence) hereafter. Further, Random Forest (RF) models were used to predict SIF and GPP and to analyse the responses of SIF and GPP to environmental drivers. The results show that both SIF and GPP variations and their relationships were dependent on the temporal scale considered. At the seasonal scale, The data show that leaf and canopy properties variations, seasonal cycle of PAR, and other abiotic factors such as VPD and SWC control not only SIF and GPP variations, but also their relationships. Further, during extreme weather conditions (heatwaves observed in 2022 in: mid-June (DOY: 166-169), mid-July (DOY: 196-199), and early August (DOY: 218-224)), we observed that SIF and reflectance-based Vegetation Indices (VIs), such as Normalized Difference Vegetation Index (NDVI) and Near-Infrared Reflectance of vegetation index (NIR_v), and also SIF and PAR are uncorrelated, while GPP, SIF, passive SIF yield (SIF_y) and active chlorophyll fluorescence yield ($F_{yieldLIF}$) strongly decreased. This indicates that during these severe abiotic conditions SIF stayed a usable proxy of GPP, while VIs cannot be used to track changes in vegetation physiology. This specific response of SIF compared to VIs underlined the interest of SIF to monitor GPP under severe abiotic conditions.

https://doi.org/10.5194/egusphere-2024-657
Preprint. Discussion started: 19 March 2024

At the diurnal timescale, the results also revealed that the saturation of the relationship between GPP and SIF was not only dependent on PAR, but also on the fraction of diffuse to total PAR, as well as on VPD, SWC, and air and canopy temperature. The other key finding was that sun geometry angles had strong effects on GPP and SIF variations. This result highlights that using ground-based SIF measurements to validate satellite measurements at coarse spatial and temporal resolutions can therefore be very difficult, due to confounding factors whose effects are significant and may vary from one site to another, especially in forest canopies.

1. Introduction

Uncertainties related to future climate forecasts are highly dependent on the terrestrial ecosystem feedback on the global carbon cycle. Vegetation carbon sequestration through photosynthesis is a main contributor to terrestrial ecosystem feedbacks (IPCC, 2022) and hence its monitoring can play a key role in global climate changes estimations. Gross Primary Production (GPP) is an indicator of vegetation carbon sequestration. GPP can be determined locally from measurements or from models (Xiao et al. 2019). However, Remote Sensing (RS) has been widely and successfully used as an unprecedented tool for upscaling, monitoring, and understanding vegetation carbon exchange across space and time (Xiao et al., 2021; Pierrat et al. 2022a).

The main success of RS observations can be attributed to their capacity in capturing valuable information on vegetation characteristics (leaf area index, chlorophyll content, fraction of absorbed radiation, surface temperature, etc.) that significantly affect or are linked to GPP. However, the relationships between RS observations and GPP are often site, and vegetation type-specific and can considerably be affected by local abiotic factors, thereby hindering the potential of this technique. Improvements in how we associate RS observations to GPP are warranted to better understand and monitor global carbon dynamics, specifically in forest ecosystems.

GPP can be described using the light-use efficiency model at canopy scale (Monteith, 1972) within Eq. (1):

$$GPP = PAR \times fAPAR \times LUE \quad (1)$$

where PAR is the flux of photosynthetically active radiation (400-700 nm), fAPAR is the fraction of PAR absorbed by the canopy, and LUE is the efficiency of the absorbed light used for photosynthesis (the fraction of absorbed light energy converted into chemical energy).

Sun-Induced chlorophyll Fluorescence (SIF) is a remotely sensed optical signal which is tightly related to photosynthesis and vegetation carbon assimilations. SIF has emerged as an unprecedented tool for monitoring GPP over a wide variety of terrestrial ecosystems (Frankenberg et al., 2011; Balde et al. 2023; Wang et al. 2020) and across diverse spatial and temporal scales (Goulas et al. 2017; Zhang et al. 2022; Pierrat et al. 2022b; Xu et al. 2021; Sun et al. 2023a) because of its links with both the canopy structure related components (mainly fAPAR) and the physiological components of GPP (i.e. LUE). Indeed, SIF can analogously be written as Eq. (2):

$$SIF = PAR \times fAPAR \times \Phi_F \times f_{esc} \quad (2)$$

where Φ_F is the fluorescence quantum yield (ratio of emitted photons to absorbed photons) and f_{esc} is the fraction of emitted SIF photons which escape the canopy to the total SIF emission. Eq. (1) and (2) showed that GPP and SIF share the same driver (i.e. Absorbed Photosynthetically Active Radiation, APAR = incident PAR x fAPAR) which have been found to explain the relationship between GPP and SIF in maize (Miao et al. 2020) and in an evergreen needleleaf forest (Kim et al. 2021). From the combination of Eq. (1) and (2), we obtain Eq. (3):

$$GPP = SIF \times \frac{LUE}{\Phi_F \times f_{esc}} \quad (3)$$

https://doi.org/10.5194/egusphere-2024-657
Preprint. Discussion started: 19 March 2024

This is the main evidence of using SIF as a proxy of GPP, notably when observations are averaged over large spatial and temporal scales (Sun et al. 2023b). However, the link between SIF and GPP is not always maintained (Damm et al. 2015; Marrs et al. 2020; Kim et al. 2021), typically when studying high temporal resolutions (diurnal level: half-hourly, hourly, etc.) or the effect of water and light limited conditions (heatwaves, drought, etc.) (Berger et al. 2022; Martini et al. 2022; Pierrat et al. 2022a). Therefore, considering a more complex relationship between SIF and GPP by taking into account temporal and spatial variations and abiotic variables could be useful to better understand GPP-SIF links.

Both SIF and GPP are affected by canopy structure (i.e. vertical distribution of LAI, clumping, canopy roughness, leaf angle distribution, etc.) and radiation conditions that mediate fAPAR and f_{esc} in time and space. At a given constant LAI, both GPP and SIF can increase under cloudy conditions as a result of increasing fAPAR because diffuse light can penetrate deeper into the canopy (Durand et al., 2021).

Besides, reflectance-based remotely sensed metrics (i.e. vegetation indices) such as the Normalized Difference Vegetation Index (NDVI, (Tucker, 1979)), the Near-Infrared Reflectance of vegetation index (NIR_v, (Badgley et al., 2017)), modified red-edge Normalized Difference Index (mNDI, (Datt, 1999)) and the Photochemical Reflectance Index (PRI, (Gamon et al., 1992)) can provide information on both structural, biochemical and functional processes that affect GPP. Indeed, VIs are also good proxies of fAPAR and hence they have been successfully used to describe canopy structure. For instance, NDVI and NIR_v provide crucial information on the structural determinants of GPP and SIF (Zeng et al. 2022). However, how these VIs are connected to changes in SIF and GPP, which are in turn heavily affected by PAR, fAPAR, changes in LUE and Φ_F, and abiotic conditions, is still unclear and need to be investigated.

The non-photochemical quenching (NPQ), a photoprotection mechanism that plants activate to avoid damage from excess light, regulates the efficiency with which APAR is used by fluorescence and photosynthesis. The extent to which plants can avoid photodamage from excess light depends heavily on the abiotic conditions and on plant photosynthetic capacity and types (Cannière et al. 2022). This is particularly important in respect to vegetation sensitivity to extreme weather conditions such as heatwaves and drought. For instance, heatwaves can create stress conditions which will affect photosynthesis and fluorescence efficiencies (Wang et al. 2022; Zanotelli et al. 2023). Thus, determining and monitoring NPQ can be crucial to provide insight into photosynthesis efficiency, and presumably also into fluorescence efficiency, even though such a relation has not been established yet. The reversible heat dissipation is the most common NPQ. It happens under short-term extreme light stress conditions and can be detected using PRI, which was found to be a good indicator of changes in photosynthesis efficiency over diurnal scales (Sukhova et al. 2022).

For instance, including information on SIF and PRI, which was used as a proxy of heat dissipation, was shown to improve GPP predictions across different vegetation types at daily scale (Wang et al. 2020). Further, Lu et al. (2020) have revealed that correcting SIF for canopy structural effects using fesc derived from NIR_v and fAPAR can also improve the relationship between SIF and GPP, underlining the relevance of disentangling structural and physiological components of SIF. It is well documented and mechanistically explained why spectral reflectance and VIs are related to changes in canopy structure at broad timescales (Zeng et al., 2022), but there is no clear evidence that there are robust relationships among them at high temporal resolutions. To establish such relationships, the canopy architecture, leaf physiology, sun-canopy geometry, and sky conditions (i.e. cloudy and sunny) have to be accounted for. Thus, the ability for VIs or reflectance-based metrics to be used as proxy of SIF

https://doi.org/10.5194/egusphere-2024-657
Preprint. Discussion started: 19 March 2024

and GPP will be limited to quantitative correlations at site-specific and vegetation type-specific, unless we are able to accurately incorporate the aforementioned effects in mechanistic models.

Recent advances in machine learning have provided opportunities for predictive modelling, data analysis, and foremostly for model output interpretation. In this context, Random Forest (RF) models are of particular interest. RF models are non-parametric and are well adapted for predicting nonlinear and multi-parameters relationships in complex situations (Breiman, 2001). RF models have already been successfully used to understand how canopy structure and functions affect the dynamics of GPP and SIF either with satellite (Balde et al. 2023) or ground-based observations (Pierrat et al. 2022a). We hypothesized that using RF models can help to understand SIF and GPP dynamics and improve their predictions based on a combination of RS metrics, radiation measurements, sun-canopy geometry and abiotic variables.

Therefore, the main concerns of this study are: 1) to understand the dynamics of GPP and SIF during a growing season and their responses to abiotic factors at diurnal and seasonal scales and 2) to predict GPP and SIF by using RF models as a quantitative and interpretative tool that can associate structural and physiological information provided by VIs, SIF (for GPP models) and abiotic variables. In this study, we used one full growing season of ground-based remote sensing data acquired in a temperate deciduous oak forest. We firstly assessed the seasonal dynamics of abiotic variables, VIs, chlorophyll fluorescence (SIF and LIF) and GPP. Secondly, we examined how abiotic factors affect the relations between GPP and SIF considering different temporal resolutions. Thirdly, we combined RS metrics and abiotic variables to predict GPP and SIF, and to quantify and interpret their contributions to GPP and SIF estimates.

2. Materials and Methods

2.1. Study site description

We collected data at the Fontainebleau-Barbeau forest site, an Eddy Covariance (EC) observation site belonging to the Integrated Carbon Observation System (ICOS) Ecosystem network (FR-Fon) (Delpierre et al. 2016). The site is located 53 km southeast of Paris, France. It is a mixed temperate deciduous broadleaf forest stand with stem density predominantly (79%) of mature sessile oak trees (Quercus petraea (Matt.) Liebl) (Maysonnave et al., 2022) and an understory of hornbeam (Carpinus betulus L.) (for more details see: http://www.barbeau.universite-paris-saclay.fr/). The climate is temperate and characterized by an annual average rainfall of approximately 680 mm and an average air temperature of approximately 11°C (Soudani et al., 2014). The LAI is approximately 5.8 $m^2.m^{-2}$ using the litter collection method (Soudani et al., 2021). At the Fontainebleau-Barbeau site, carbon and water fluxes have been continuously monitored at 35 m height using the EC method.

2.2. Data collection: ground-based remote sensing, GPP, and environmental variables

Ground-based remotely sensed observations (far-red SIF, NDVI, NIR_V, PRI, mNDI, and spectral reflectance) were collected using an automated instrument (named SIF3) and developed thanks to a collaboration between the "Laboratoire de Météorologie Dynamique (LMD), École Polytechnique, France and Laboratoire Écologie, Systématique et Évolution, Université Paris-Saclay, France". The automated instrument SIF3 was installed above the canopy at the top of a 35 m height tower of the Fontainebleau-Barbeau site. To avoid additional shading from the tower on the measured area, the SIF instrument was set to the southern part of the tower. It has a 25° field of

https://doi.org/10.5194/egusphere-2024-657
Preprint. Discussion started: 19 March 2024

view (FOV) and measures alternatively the sun irradiance and the vegetation radiance at a high spectral resolution (0.3 nm) to deduce SIF, spectral reflectance, and VIs (Balde et al., 2023a). In this study, observations run from April 2022 to mid-September 2022. Remotely sensed observations were averaged over a 30 min window synchronized with GPP and abiotic variables that are also recorded every 30 min. Far-red SIF (i.e. at 760 nm) was retrieved using a Fraunhofer-line based retrieval method (Daumard et al. 2012). This method has been widely used for SIF retrieval because of its lower sensitivity to atmospheric scattering and its reliability even under cloudy sky conditions (Mohammed et al. 2019; Cendrero-Mateo et al. 2019). Low quality retrieval and retrieval with unstable illumination conditions were filtered out from SIF observations.

Active chlorophyll fluorescence ($F_{yieldLIF}$) measurements, which allowed to assess directly variations in vegetation physiology, were acquired with a fluorometer, named LIF, developed at the LMD laboratory, which was also installed above the canopy at the top of the 35 m height tower next to SIF3. This instrument is similar to the one described by Moya et al. (2019). It uses a powerful blue LED array (ENFIS Ltd, Swansea, UK; peak wavelength 455 nm, FWHM 25 nm, radiant power 6 W) as an excitation source. The optical head consisted of two main parts: (i) the excitation source module that includes the blue LED array driven by a laboratory-made (LMD, Ecole Polytechnique) electronic system stabilizing the pulse peak power (electrically and optically), a heat dissipation module and a Fresnel lens (diameter 180 mm) to collimate the excitation light, and (ii) a detection module that includes a second Fresnel lens with the same diameter, a set of optical filters, a large area PIN photodiode (10x10 mm^2, S3590, Hamamatsu Photonic, Japan) and a laboratory-made (LMD) amplifier that selects the LED induced fluorescence signal ($F_{yieldLIF}$) from the reflected sunlight in the same wavelengths band (LNIR The FOV can be controlled thanks to an onboard camera (RLC-520A, Reolink, Hong-Kong). We selected a top of the canopy area in the FOV of the SIF instrument, resulting in a 9 m measuring distance with a viewing zenith angle of 30°. However, as the FOV of the instrument is about 100 mrad, the measured area was about 0.4 m^2, which is much smaller than the FOV of SIF3 (approximately 6 m^2). For more details on the instrument principale, we referred the reader to (Balde et al., 2023a). Note that LIF measurements were also averaged at 30 min.

The VIs, namely NDVI and NIR_v as indicators of vegetation structure, mNDI as an indicator of leaf chlorophyll content, and PRI as an indicator of extreme heat dissipation, were calculated as follow:

$$NDVI = \frac{R_{[780-800]} - R_{[670-680]}}{R_{[780-800]} + R_{[670-680]}} \quad (4)$$

$$NIR_v = R_{[780-800]} \times NDVI \quad (5)$$

$$mNDI_{705} = \frac{R_{750} - R_{705}}{R_{750} + R_{705} - 2 \times R_{445}} \quad (6)$$

$$PRI = \frac{R_{[569-571]} - R_{[520-532]}}{R_{[569-571]} + R_{[520-532]}} \quad (7)$$

with R being the reflectance at a given wavelength or the average across a wavelength range in nm.

To consider the physiological component of SIF, an apparent fluorescence yield (SIF_y) was calculated by normalizing SIF by PAR. We used half-hourly GPP data estimated from net ecosystem EC gas exchanges measurements. GPP and SIF data were also aggregated at daily timescale to study the seasonal dynamics. The main micrometeorological variables, including incident, direct, and diffuse radiations in the PAR spectral range, were measured at a high frequency (1 min) and were aggregated at the half-hourly and the daily temporal resolutions. Atmospheric Vapor Pressure Deficit (VPD), precipitation (P), air (T_a) and canopy (T_{canopy}) temperatures, and Soil Water Content (SWC) were recorded half-hourly and were averaged at daily scale. Note that the SWC are averaged values in cm^3 water per cm^3 soil, calculated between 0 and 150 cm depth.

https://doi.org/10.5194/egusphere-2024-657
Preprint. Discussion started: 19 March 2024

To consider the effects of the sky, the fraction of diffuse radiation over the total incoming radiation was determined. This fraction varies with respect to variations in sun zenith angle and with sky conditions. It is worth noting that values of the fraction < 0.3 are considered as sunny days and values of the fraction > 0.70 as cloudy days.

3. Data analysis: seasonal dynamics, GPP vs SIF relationships, and random forest models

The influence of environmental variables on the links between GPP and SIF was examined at daily and seasonal timescales using a non-linear curve fitting of GPP vs SIF (Kim et al. 2021) and a linear model of GPP vs SIF. The coefficient of determination (R^2) was used to assess the strength of the correlations.

We examined the significance of remote sensing metrics (reflectance and VIs), sun-canopy geometry, and abiotic variables as predictors for SIF and GPP at diurnal scale using RF regression models. Various types of RF models were established for estimating SIF and GP (Table 1). All RF models were created using 200 trees and sampled with replacement based on bag fraction of 80% (80% of the data for training and 20% for testing). All RF models were run with only sunny days data at a half-hourly temporal resolution. The out-of-bag (OOB) predictor importance estimates were determined to evaluate the contribution of each predictor to the predicted output. Conversely to predictor importance estimates, partial dependence plots allow to examine the relationship between inputs (predictors) and predicted variables (i.e. GPP or/and SIF) within the predictor's range of variability. Therefore, the partial dependence plots were used to study the relationship between inputs and GPP or/and SIF. Model performance was evaluated using the OOB R^2 score and the adjusted R^2 between the testing dataset and the predictions, as well as the Root Mean Squared Error (RMSE). The closest the OOB R^2 and adjusted R^2 are, the better the model is able to be generalized.

Table 1. Random forest models set up for SIF and GPP predictions using environmental and remote sensing variables as inputs with only sunny days data: Photosynthetically Active Radiation (PAR), atmospheric Vapor Pressure Deficit (VPD), volumetric Soil Water Content (SWC), Sun Azimuth Angle (SAA), far-red Sun-Induced chlorophyll Fluorescence (SIF) at 760 nm, Photochemical Reflectance Index (PRI), Near-Infrared Reflectance of vegetation index (NIR_V), Normalized Difference Vegetation Index (NDVI), and modified red-edge Normalized Difference Index (mNDI).

Model name	Inputs	Outputs	Purpose
GPP-ENV-SA	VPD, SWC, PAR, SAA	GPP	To test the synergy between environmental variables and sun angles to predict GPP.
GPP-ENV-RS	SIF, PRI, NIR_V, NDVI, mNDI, VPD, SWC, PAR, SAA	GPP	To test the synergy between remote sensing, environmental variables and sun angles to predict GPP.
SIF-ENV-SA	VPD, SWC, PAR, SAA	SIF	To test the synergy between environmental variables and sun angles to predict far-red SIF.
SIF-ENV-RS	PRI, NIR_V, NDVI, mNDI, VPD, SWC, PAR, SAA	SIF	To test the synergy between remote sensing, environmental variables and sun angles to predict far-red SIF.

4. Results

4.1. Seasonal variations in GPP, SIF, VIs and environmental variables

The variations in GPP, SIF, $F_{yieldLIF}$, SIF_y, VIs, and abiotic variables at the Fontainebleau-Barbeau forest site during the period of measurements (growing season 2022) are illustrated in Figure 1.

The GPP of the Fontainebleau-Barbeau forest started to raise gradually in April after the budburst and until almost the end of May following the development of the leaves and the increase in solar radiation (Figure 1A). Seasonal variations in GPP were characterized by sharp fluctuations across the season reflecting PAR, T_a, and VPD changes.

https://doi.org/10.5194/egusphere-2024-657
Preprint. Discussion started: 19 March 2024

The dynamics in Ta and VPD (Figure 1J and 1K) showed contrasted and marked weather conditions (i.e. in 2022 summer in Barbeau, heatwaves in: mid-June (DOY: 166-169), mid-July (DOY: 196-199), and early August (DOY: 218-224)), coinciding to the peak values of Ta and VPD. Note that during these heatwaves' periods, GPP substantially decreased and the values of Ta and VPD showed obvious air drought conditions. The seasonal variations in SWC (Figure 1L) revealed an overall steady decline, meaning that the soil was constantly drying from an SWC > 0.4 cm^3 cm^{-3} at the beginning of the season to an SWC < 0.27 cm^3 cm^{-3} in the end.

The seasonal variations in NDVI an indicator of leaf area index, and mNDI an indicator of leaf chlorophyll pigments, exhibited similar patterns, which represent the seasonality changes of canopy attributes in deciduous forests (Figure 1E and 1G). PRI values showed a rapid increase during the budburst and the leaf expansion phases until it reached its maximum in late May (Figure 1H). Afterwards, PRI is stable and slightly decreased during the leaf maturation phase. This PRI temporal pattern was consistent with the temporal pattern of NDVI and mNDI throughout the season. The within-day PRI changes are attributable to the activity of the xanthophyll cycle and to fluctuations in the PAR intensity, while the seasonal dynamic of NIR_v (Figure 1F) was due to day-to-day changes in light intensity and sun-canopy geometry, and also to changes in canopy attributes throughout the season.

Far-red SIF followed the same temporal pattern as the other variables (Figure 1B), reflecting the phenological dynamics of the canopy. Like GPP, far-red SIF reached its maximal values soon after the new leaves were fully developed. The SIF curve showed a plateau until mid-July and then gradually declined following the decrease in GPP. $F_{yieldLIF}$ showed a steady decrease over the season (Figure 1C), while variations in SIF_y (Figure 1D) were driven by the changes in light intensity and indicated the onset of the growing season. The dynamics in SIF_y also showed a similar trend of decrease across the season like GPP and SIF. Note that both $F_{yieldLIF}$ and SIF_y significantly declined during the heat waves periods, as it has been observed in GPP and SIF dynamics. But, vegetation attributes such as NDVI and mNDI were not significantly affected during these summer heatwaves. This underlines the growing interest of using SIF as a proxy of GPP under severe abiotic conditions at the ecosystem scale.

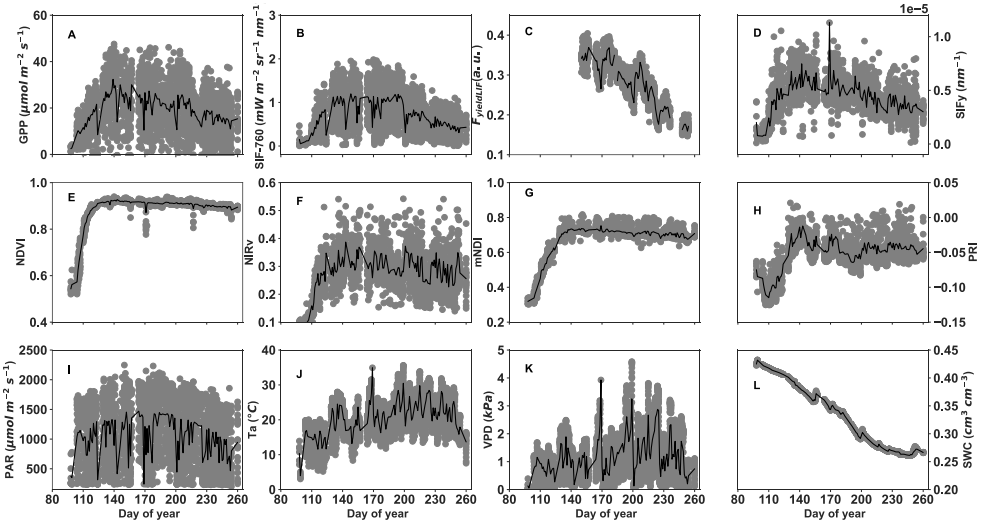

Figure 1. Variations in Gross Primary Production (GPP) (Figure 1A), far-red Sun-Induced chlorophyll Fluorescence (SIF) of the canopy (Figure 1B), active chlorophyll fluorescence yield ($F_{yieldLIF}$) (Figure 1C), apparent SIF yield (SIF_y) (Figure1D), Normalized Difference Vegetation Index (NDVI) (Figure 1E), Near-Infrared Reflectance of vegetation index (NIR_v) (Figure

https://doi.org/10.5194/egusphere-2024-657
Preprint. Discussion started: 19 March 2024

1F), modified red-edge Normalized Vegetation Index (mNDI) (Figure 1G), Photochemical Reflectance Vegetation Index (PRI) (Figure 1H), Photosynthetically Active Radiation (PAR) (Figure 1I), air temperature (Ta) (Figure 1J), Vapor Pressure Deficit (VPD) (Figure 1K), and volumetric Soil Water Content (SWC) (Figure 1L) under all sky conditions during the 2022 growing season. Gray points indicate the data at half-hourly timescale and the black line represents daily mean values.

4.2. Influence of abiotic variables on the daily and seasonal variations of the relationship between GPP and SIF

Considering all the data acquired, the relationship between GPP and SIF was non-linear (Figure 2). The relationship between GPP and SIF is hyperbolic. The hyperbolic regression yields a significantly higher $R^2 = 0.53$ than a linear regression at half-hourly time resolution (Figure 2A). The results also reveal that the relation between GPP and SIF is significantly stronger for cloudy days than for sunny days, with R^2 of 0.66 and 0.59, respectively (data not shown).

The relationship between SIF and GPP exhibits gradual changes with the day of year (DOY), the PAR (Figure 2B), the fraction of diffuse to total PAR (Figure 2C), the VPD (Figure 2D), the T_{canopy} (Figure 2E), and the SWC (Figure 2F). It can be seen that the saturation of GPP with increasing SIF was determined by high PAR, VPD and T_{canopy}. In other words, the ratio GPP over SIF decreases with increasing PAR, VPD, and T_{canopy}. Time (DOY), reflecting the seasonal dynamic, has a strong impact on the relationship between SIF and GPP: both GPP and SIF increased linearly from the start of the season until around DOY 140, afterward GPP started saturating until around DOY 215, and then both GPP and SIF linearly decreased. This underlines the fact that seasonal variations in leaf and canopy characteristics have a large influence on the relationship between SIF and GPP (Figure 2B). The changes in the fraction of diffuse to total PAR also reveals that The R^2 between SIF and GPP increased on contrasting days of clear and overcast skies (Figure 2C and Figure 3B). However, on sunny days, GPP showed saturation, when SIF continued to increase. Finally, the SWC has also an influence on the relationship between GPP and SIF, with drier conditions corresponding to the lowest GPP and SIF values and the highest GPP and SIF values observed when water availability was not a limiting factor (Figure 2F).

https://doi.org/10.5194/egusphere-2024-657
Preprint. Discussion started: 19 March 2024

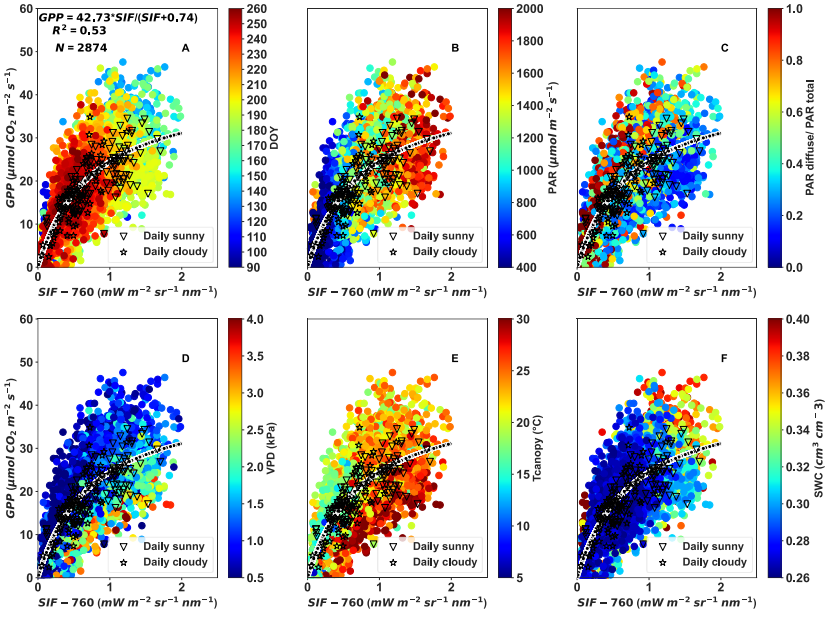

Figure 2. The hyperbolic relationship between Gross Primary Production (GPP) and far-red Sun-Induced chlorophyll Fluorescence (SIF) at half-hourly timescale seen with color scaled dots for: day of year (DOY, Figure 2A), Photosynthetically Active Radiation (PAR, Figure 2B), ratio of diffuse to total PAR (Figure 2C), Vapor Pressure Deficit (VPD, Figure 2D), leaf canopy temperature (Tcanopy, Figure 2E), and mean Soil Water Content at 150 cm depth (SWC, Figure 2F), except data represented in triangles and stars points.

In Figure 3 the coefficient of determination (R^2) of the relation between daily GPP and daily SIF shows strong inter-daily variability. R^2 generally decreases when VPD (Figure 3C) and PAR (Figure 3A) are high. The highest correlations were obtained for relatively low VPD and moderate PAR, and during cloudy days (Figure 3B). this decline was markedly during the summer heatwaves in 2022. This suggests that inter-daily variations in GPP and SIF relations were significantly affected by the abiotic conditions, as well as by the intermittence between cloudy and sunny periods.

https://doi.org/10.5194/egusphere-2024-657
Preprint. Discussion started: 19 March 2024

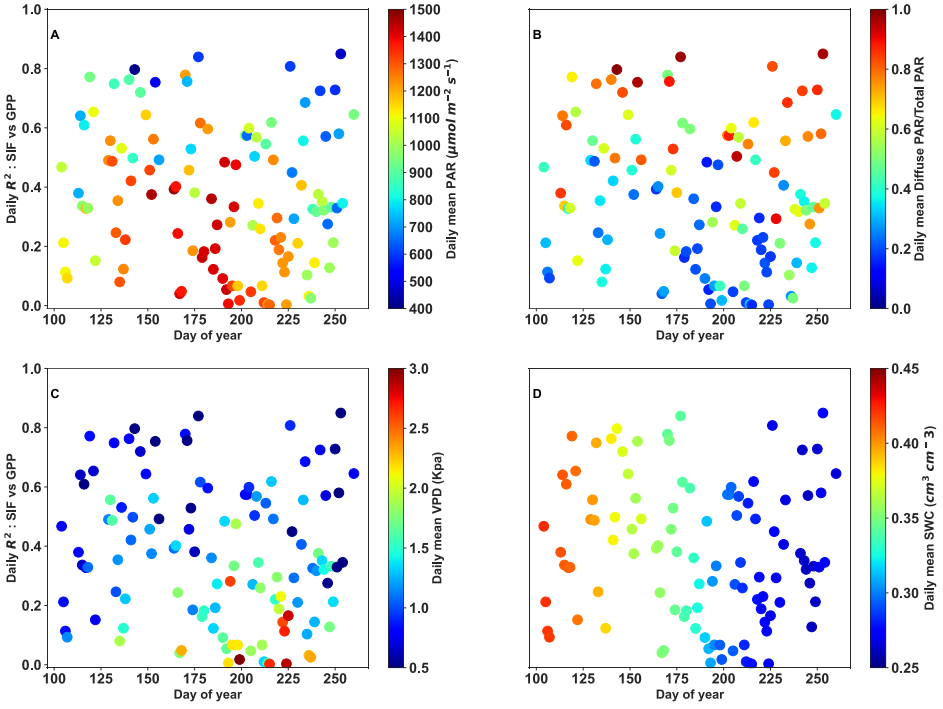

Figure 3. Inter-daily variations of the coefficient of determination (R^2) of the linear relation between GPP vs far-red SIF seen with color scaled dots for: Photosynthetically Active Radiation (PAR, Figure 3A), ratio of diffuse to total PAR (Figure 3B), Vapour Pressure Deficit (VPD, Figure 3C), and Soil Water Content (SWC, Figure 3D). The number of data points per day varied between 20 and 23, representing more than 87% of the total data points.

How GPP is related to SIF at satellite overpass times is a crucial question. Hence, we investigated the relationship between GPP and SIF at satellite overpass times using only data acquired at 10H30 am and 13H30 pm on sunny days (Figure 4). A substantial hyperbolic relation was found between GPP and far-red SIF at satellite overpass times. The results presented in Figure 4 showed that the non-linear correlation was stronger in the afternoon (13h30 pm) than in the morning (10h30 am) with R^2 of 0.79 and 0.57, respectively. This suggests that the GPP-SIF relation depends strongly on the vegetation physiological state and on the conditions of illumination.

https://doi.org/10.5194/egusphere-2024-657
Preprint. Discussion started: 19 March 2024

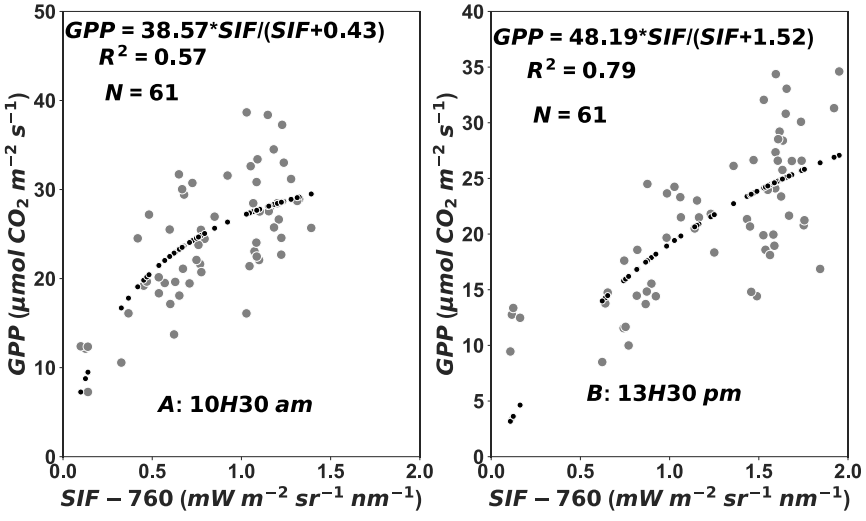

Figure 4. Relationship between daily GPP and daily far-red SIF (SIF-760) at satellite overpass times on sunny days. R^2 represents the coefficient of determination and the hyperbolic regression line is the black dotted line.

4.3. Main drivers of SIF and GPP variations and predictions on sunny days

To predict GPP and SIF using environmental and remote sensing variables and assess the contribution of these variables to their variations, several RF regression analyses (Table 1) were performed and the main results are presented in Figures 5, 6, and 7 (the other model results are given in Supplementary materials Figures S1, S2 and S3). The predictor importance estimates for SIF-ENV-RS model is exhibited in Figure 5B. This model explains approximately 94% of the total variance of far-red SIF (Figure 5A). SWC appears to be the most important variable, followed by PAR and SAA, and the contribution of mNDI, PRI, and VPD play lesser roles for SIF prediction (Figure 5B). For GPP, the RF model represented in Figure 5D captures between 69% and 72% of the variability in GPP (Figure 5C). VPD and SAA appear to be the most determinant variables, followed by SWC, far-red SIF, PAR and NDVI, and the contribution of all other variables was relatively minor for GPP prediction.

https://doi.org/10.5194/egusphere-2024-657
Preprint. Discussion started: 19 March 2024

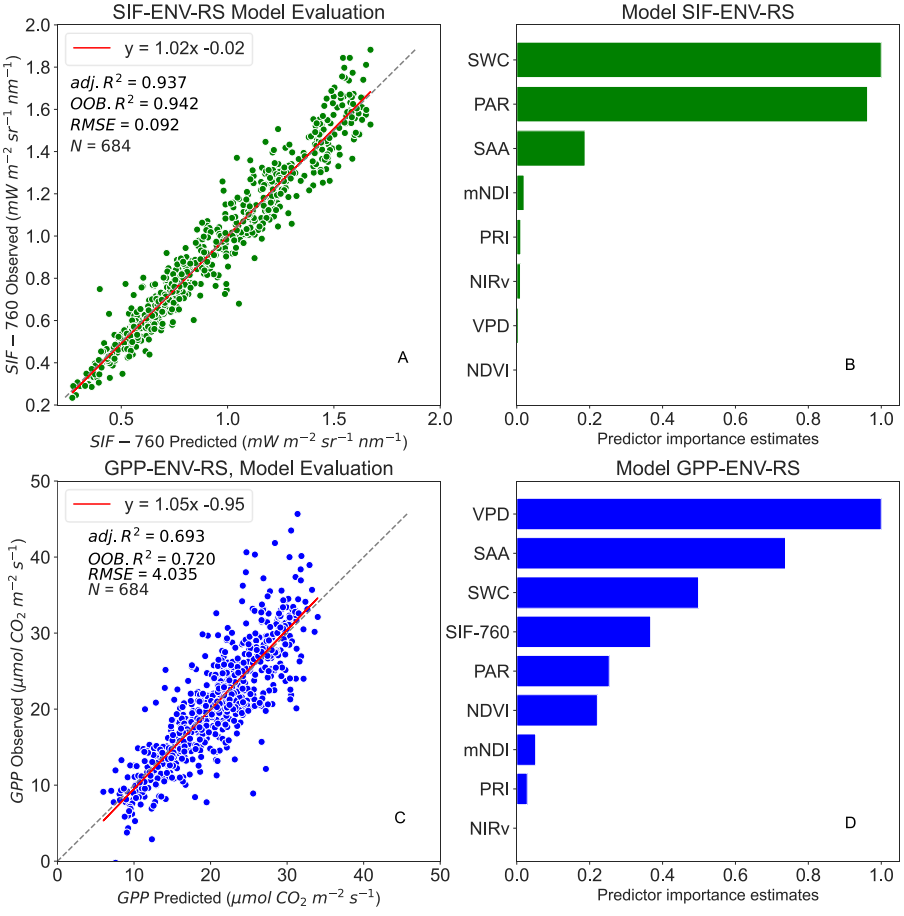

Figure 5. Figure 5A presents SIF-ENV-RS model performance between observed and predicted SIF (SIF-760), Figure 5B shows predictor importance estimates for SIF-ENV-RS model, Figure 5C presents GPP-ENV-RS model performance between observed and predicted GPP, Figure 5D shows predictor importance estimates for GPP-ENV-RS model. N denotes the number of observations used for the RF model evaluation, adj. R^2 represents the adjusted coefficient of determination of the relationship between observed and predicted SIF or GPP (validation data), OOB R^2 is the model accuracy on the validation data, and the RMSE is the root mean square error between observed and predicted SIF or GPP. The dashed diagonal line depicts the 1:1 line. Data at half-hourly timescale on only sunny days were used.

The partial dependence in a machine learning model plot is a visual representation that allows to understand the relationship between a specific feature or variable (inputs) and the predicted outcome (target variable) while holding all other features constant over the whole range of predictor's variability, oppositely to the variable importance estimates showing only the contribution or importance of the inputs to the prediction. The results in Figures 6 and 7 show how the predicted SIF and GPP changes as the SWC or VPD or PAR varies, while keeping other features constant. In these figures (6 and 7), we can observe that SIF and GPP demonstrated similar responses to the three abiotic factors (SWC, VPD and PAR) variations. Both SIF (Figure 6) and GPP (Figure 7) respond positively when SWC increases to a SWC level of around 30%, then the GPP responds more slowly and SIF saturates at high SWC values. It can also be seen that overall the relationships between SIF and VPD (Figure 6) and GPP and VPD (Figure 7) are negative, but an average the magnitude of SIF (average SIF) and GPP (average GPP) showed less variations, due to likely to the observed few days of heatwaves in the summer of 2022. Last but

https://doi.org/10.5194/egusphere-2024-657
Preprint. Discussion started: 19 March 2024

not least, the relations between SIF and PAR are strictly positive and present overall less variabilities (color code in green), while the relationships between GPP and PAR saturate at high PAR values (PAR > 1500 µmol m^{-2} s^{-1}) and show high variations or uncertainties (color code in blue). However, it is worth mentioning that an average the magnitude of SIF and GP is comparable for SWC and PAR variables, underlining the link between the seasonal patterns in SIF or/and GPP and SWC or/and PAR variations.

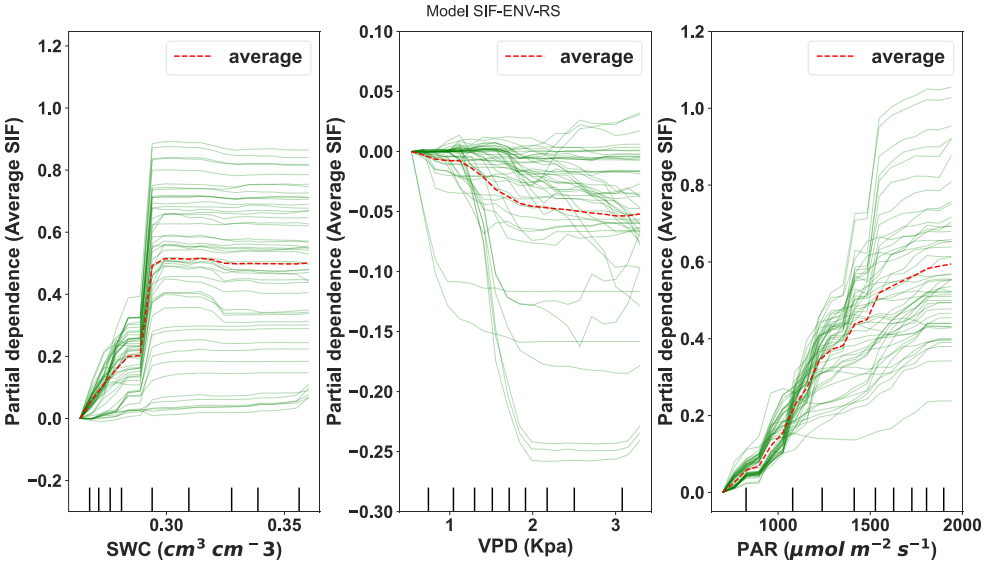

Figure 6. Partial dependence describing the effect of each variable on far-red SIF variations for clear sky days at half-hourly timescale.

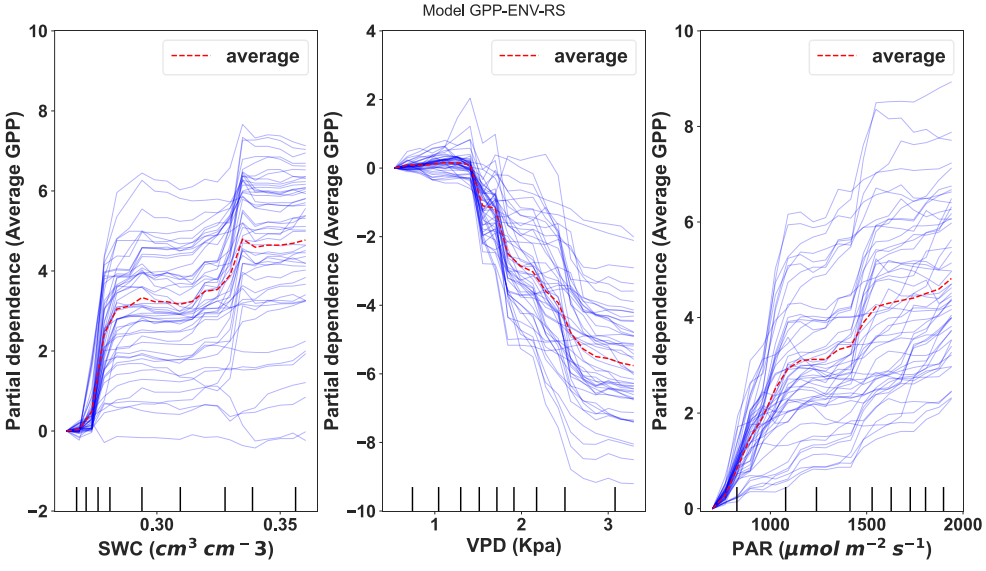

Figure 7. Partial dependence describing the effect of each variable on GPP variations for clear sky days at half-hourly timescale.

https://doi.org/10.5194/egusphere-2024-657
Preprint. Discussion started: 19 March 2024

4.4. Discussion

The results highlight that the seasonal patterns of SIF and GPP are similar (Figure 1), indicating that the temporal changes of both SIF and GPP are primarily driven by the seasonal changes in canopy structure and solar radiation conditions. Variations in vertical distribution of LAI, leaf angle distribution and clumping, and light intensity strongly determine the amount of APAR. The seasonal changes also affect leaf biochemical properties and the distribution of sunlit and shaded leaves on which SIF and GPP depend (Lu et al., 2020; Zhang et al., 2023). Besides, leaf physiology and abiotic factors (mainly leaf canopy temperature, VPD, and SWC) considerably affected the seasonal dynamics in $F_{yieldLIF}$ and SIF_y, and consequently the dynamics of SIF and GPP. These results are consistent with previous studies at both leaf and canopy scales (Lu et al. 2020; Kováč et al. 2022; Hu et al. 2023). The data in Figure 1 also demonstrated that seasonal changes in PRI and NIR_v were consistent with the dynamics of NDVI and mNDI throughout the season, indicating their dependence on the seasonal cycle of canopy. Note that short-terms variations in PRI and NIR_v were greater than those in NDVI and mNDI, suggesting that these indices are relatively independent at short timescale (intra-daily). In fact, short timescale variations in PRI may be related to the activity of xanthophyll cycle and fluctuations in light intensity as it has been shown in previous studies (Hmimina et al. 2014; Soudani et al. 2014; Sukhova et al. 2022). However, the seasonal dynamic in NIR_v is substantially affected by canopy structure (LAI) and sun-canopy geometry changes that determine the fraction of sunlit and shaded leaves (Zhang et al. 2022; Zeng et al. 2022). Finally, during the heatwaves mid-June (DOY: 166-169), mid-July (DOY: 196-199), and early August (DOY: 218-224), we observed that SIF and VIs (NDVI, NIR_v, mNDI, and PRI) and SIF and PAR are uncorrelated, while both GPP and SIF strongly decreased. This indicates that SIF can capture, at least partially, the vegetation functioning activity and that VIs cannot be used to monitor changes in vegetation physiology during severe abiotic conditions. This specific response of SIF compared to VIs underlined the interest of SIF as a proxy of GPP under severe abiotic conditions. Note that $F_{yieldLIF}$ and SIF_y also significantly dropped during the heatwaves periods, underlining the ability of $F_{yieldLIF}$ and SIF to reflect variations in vegetation physiology functioning under extreme weather conditions.

At the half-hourly temporal resolution, when SIF and GPP were considerably affected by variations in PAR (Figure 2), the relationship between GPP and SIF was strongly non-linear. This result suggests that the chlorophyll fluorescence does not linearly co-vary with photosynthesis because GPP saturates at a high PAR, while fluorescence continues to increase with PAR as demonstrated by the partial dependence correlations in Figures 6 and 7. This finding is consistent with several previous studies (Helm et al. 2020; Cheng et al. 2022; Sun et al. 2023b). This study also underlines that the hyperbolic relations between GPP and SIF was better on cloudy days ($R^2 = 0.66$) than on sunny days ($R^2 = 0.59$), indicating that light intermittence within and over the canopy and sun-canopy geometry significantly affected the link between GPP and SIF. These findings are in good agreement with previous studies in cork oak forest (Cheng et al. 2022). Clouds reduce the total sun radiation received over the canopy and increase the diffuse radiation. Canopy SIF is mainly affected by direct radiation and is less impacted by diffuse radiation than GPP (Sun et al., 2023b). Further, diffuse radiation can penetrate deeper in the canopy, presumably inducing more SIF emission due to shaded leaves emission's and greatly reducing sun-canopy geometry effects. However, under high light intensity, which is clearly more frequent on sunny days, the excess absorbed light is dissipated as heat inducing both a decrease in the photosynthetic activity and the SIF emission. This is because when light intensity increases, the carbon assimilation and the electron transport chain gradually become light saturated (Porcar-Castell et al. 2014). This explains why the link between GPP and SIF at satellite

https://doi.org/10.5194/egusphere-2024-657
Preprint. Discussion started: 19 March 2024

overpass times evidenced that GPP and SIF were hyperbolically more related in the afternoon (13H30 pm) than in the morning (10H30 am) (Figure 4). Further, under high and changing light conditions, GPP is sensitive to circadian rhythms, meaning that photosynthesis light saturation is more important in the afternoon than in the morning (Li et al., 2023).

If the light saturation of GPP is the primary widely known driver in the discrepancy between GPP and SIF, there are abiotic variables that vary intra-daily, daily and seasonally. These variables may have significant effects on the fluorescence efficiency and the photosynthetic activity and consequently they can affect the relationship between GPP and SIF. Thus, the results presented here (in Figures 2, 3 and 5) evidenced that T_{canopy}, SWC and VPD are all influencing GPP and SIF. Therefore, they may be responsible for intra-daily and seasonal divergence in the GPP-SIF relationship. More specifically, strong discrepancies between GPP and SIF were associated with high PAR, T_{canopy}, and VPD (Figures 2 and 3). Previous studies have also identified PAR and VPD as potential causes for the non-linearity between GPP and SIF (Kim et al. 2021; Hu et al. 2023). In addition, abiotic variables can impact SIF and GPP at several levels. The abiotic variables can affect the light energy partitioning in the photosynthetic apparatus, leading to NPQ activation. VPD is an indicator of atmospheric water demand and in this study VPD reached values that corresponded to severe air drought during the heatwaves that occurred in the summer in 2022. Air drought can also affect stomatal closure. Stomatal closure can lead to decrease in plant water use efficiency and can prevent carbon assimilation and can inhibit the electron transport chain activity (Jonard et al. 2020; Magney et al., 2020), hence, affecting photosynthesis and fluorescence emission and consequently the relationship between GPP and SIF (Figures 3 and 5). This behavior might be observed in our results (Figures 2, 3 and 5). Previous studies has also demonstrated that the influence of the VPD on the SIF-GPP relationship had a critical effect (Cheng et al. 2022). More specifically, we observed that a high VPD had a negative effect on both GPP and SIF (Figures 6 and 7). We also observed that both GPP and SIF saturate at high SWC (Figures 6 and 7). The SWC is an indicator of plant water stress which affects stomatal closure and hence the light reaction of photosynthesis and the fluorescence. The SWC was shown to have different responses to SIF and GPP in cork oak and poplar trees (Cheng et al. 2022), suggesting the relation of GPP and SIF with SWC may be also vegetation type-specific. The positive relationships between SIF and PAR indicate that the seasonal changes in PAR control variations in SIF at the canopy scale. Whereas, the saturation of GPP with increasing PAR is associated with the saturation of carbon assimilation in leaves under high light intensity. Therefore, this study supports that field measurements of remote sensing metrics, ecosystems and abiotic variables are needed to better understand the dynamics of GPP and SIF and their relationship.

4.5. Conclusion

In this study, the concomitant and continuous measurements of Sun-Induced chlorophyll Fluorescence, Gross Primary Production, reflectance-based vegetation indices and abiotic variables of a sessile oak canopy allowed to analyse the main drivers of SIF and GPP variations. On one hand, the seasonal variations in SIF, GPP, VIs, and abiotic variables (including PAR, air and canopy temperatures, Soil Water Content and Vapor Pressure Deficit) were examined, and on the other hand, the relationships between GPP and SIF was evaluated considering different temporal resolutions. Further, Random Forest models were also used to not only predict SIF and GPP, but also to analyse the responses of SIF and GPP to abiotic drivers.

https://doi.org/10.5194/egusphere-2024-657
Preprint. Discussion started: 19 March 2024

The results showed that both SIF and GPP had similar seasonal patterns, which were primarily controlled by the vegetation phenology (canopy structure and leaf biochemical and physiological attributes) and diurnal and seasonal changes in incoming solar radiation. The analyses also demonstrated that the saturation of the relationship between GPP and SIF was not only dependent on PAR, but also on the fraction of diffuse to total PAR and on other abiotic variables such as VPD, SWC, and canopy temperature. The other key finding was that sun geometry angles had strong effects on GPP and SIF, suggesting that sun-canopy geometry effects impact the relationship between GPP and SIF. This last result may be specific to our study site consisting of a mature forest which has a complex structure, but it clearly highlights that the use of passive SIF measurements acquired at the canopy scale with a narrow field of view must be conducted with great care, as the measurements are strongly impacted by the distribution of sunlit and shaded leaves at the top of the canopy. Using in-situ ground SIF measurements to validate satellite measurements at coarse spatial and temporal resolutions can therefore be difficult, since obtained results will not be the same from one site to another, particularly in forest canopies where the structure is highly heterogeneous. Alternative solutions based on active chlorophyll fluorescence measurements at canopy scale, or airborne measurements that take account of canopy heterogeneity, need to be considered.

Code and data availability: The computer codes (MATLAB and Python) used in this study are available from the corresponding author upon request.

Supplement: The supplementary materials related to this manuscript is available as a pdf document.

Author contributions: conceptualization, All co-authors; methodology, H.B., G.H., Y.G. and K.S.; instruments design and development Y.G., A.O., G.L., G.H., K.S., D.B.; software H.B. and G.H.; validation, H.B.; formal analysis, H.B., G.H., Y.G. G.L., and K.S.; investigation, H.B., G.H., Y.G. G.L., and K.S.; resources, H.B., G.H., Y.G. and K.S.; data curation, H.B. and G.H.; writing-original draft preparation, H.B.; writing reviewing and editing, all co-authors; visualization, H.B.; supervision, K.S., Y.G., G.H., and G.L.; project administration, Y.G. and K.S.; funding acquisition, Y.G. and K.S.; All authors have read and agreed to the final version of the manuscript.

Competing interests: The authors declare that they have no conflict of interest.

Funding: This PhD work was jointly funded by the “Centre National d'Études Spatiales” (CNES) and ACRI-ST (Toulouse, France) (contract CNES-ACRI-ST-Ecole polytechnique-CNRS n°3425). This work was also supported by CNES through the VELIF project focused on the FLEX mission (contracts 4500073234 and 4500073501), The “Program National de Télédétection Spatiales” (PNTS) across the C-FLEX project and EIT Climate-KIC project via the Agriculture Resilience, Inclusive, and Sustainable Enterprise (ARISE) project (EIT 190733).

Acknowledgements: The authors thank Nicolas Delpierre, Alexandre Morfin, and Clotilde Pérot-Guillaume for their participation on data acquisition and management at the Barbeau forest site.

https://doi.org/10.5194/egusphere-2024-657
Preprint. Discussion started: 19 March 2024

References

Badgley, G., Field, C. B., and Berry, J. A.: Canopy near-infrared reflectance and terrestrial photosynthesis, Science Advances, 3, e1602244, https://doi.org/10.1126/sciadv.1602244, 2017.

Balde, H., Hmimina, G., Goulas, Y., Latouche, G., Ounis, A., and Soudani, K.: Data-based investigation of the effects of canopy structure and shadows on chlorophyll fluorescence in a deciduous oak forest, Remote Sensing: Terrestrial, https://doi.org/10.5194/egusphere-2023-2419, 2023a.

Balde, H., Hmimina, G., Goulas, Y., Latouche, G., and Soudani, K.: Synergy between TROPOMI sun-induced chlorophyll fluorescence and MODIS spectral reflectance for understanding the dynamics of gross primary productivity at Integrated Carbon Observatory System (ICOS) ecosystem flux sites, Biogeosciences, 20, 1473–1490, https://doi.org/10.5194/bg-20-1473-2023, 2023b.

Berger, K., Machwitz, M., Kycko, M., Kefauver, S. C., Van Wittenberghe, S., Gerhards, M., Verrelst, J., Atzberger, C., van der Tol, C., Damm, A., Rascher, U., Herrmann, I., Paz, V. S., Fahrner, S., Pieruschka, R., Prikaziuk, E., Buchaillot, Ma. L., Halabuk, A., Celesti, M., Koren, G., Gormus, E. T., Rossini, M., Foerster, M., Siegmann, B., Abdelbaki, A., Tagliabue, G., Hank, T., Darvishzadeh, R., Aasen, H., Garcia, M., Pôças, I., Bandopadhyay, S., Sulis, M., Tomelleri, E., Rozenstein, O., Filchev, L., Stancile, G., and Schlerf, M.: Multi-sensor spectral synergies for crop stress detection and monitoring in the optical domain: A review, Remote Sensing of Environment, 280, 113198, https://doi.org/10.1016/j.rse.2022.113198, 2022.

Breiman, L.: Random Forests, Machine Learning, 45, 5–32, https://doi.org/10.1023/A:1010933404324, 2001.

Cendrero-Mateo, Wieneke, Damm, Alonso, Pinto, Moreno, Guanter, Celesti, Rossini, Sabater, Cogliati, Julitta, Rascher, Goulas, Aasen, Pacheco-Labrador, and Arthur: Sun-Induced Chlorophyll Fluorescence III: Benchmarking Retrieval Methods and Sensor Characteristics for Proximal Sensing, Remote Sensing, 11, 962, https://doi.org/10.3390/rs11080962, 2019.

Cheng, X., Hu, M., Zhou, Y., Wang, F., Liu, L., Wang, Y., Huang, H., and Zhang, J.: The divergence of micrometeorology sensitivity leads to changes in GPP/SIF between cork oak and poplar, Agricultural and Forest Meteorology, 326, 109189, https://doi.org/10.1016/j.agrformet.2022.109189, 2022.

Damm, A., Guanter, L., Paul-Limoges, E., van der Tol, C., Hueni, A., Buchmann, N., Eugster, W., Ammann, C., and Schaepman, M. E.: Far-red sun-induced chlorophyll fluorescence shows ecosystem-specific relationships to gross primary production: An assessment based on observational and modeling approaches, Remote Sensing of Environment, 166, 91–105, https://doi.org/10.1016/j.rse.2015.06.004, 2015.

Datt, B.: A New Reflectance Index for Remote Sensing of Chlorophyll Content in Higher Plants: Tests using *Eucalyptus* Leaves, Journal of Plant Physiology, 154, 30–36, https://doi.org/10.1016/S0176-1617(99)80314-9, 1999.

Daumard, F., Goulas, Y., Champagne, S., Fournier, A., Ounis, A., Olioso, A., and Moya, I.: Continuous Monitoring of Canopy Level Sun-Induced Chlorophyll Fluorescence During the Growth of a Sorghum Field, IEEE Transactions on Geoscience and Remote Sensing, 50, 4292–4300, https://doi.org/10.1109/TGRS.2012.2193131, 2012.

De Cannière, S., Vereecken, H., Defourny, P., and Jonard, F.: Remote Sensing of Instantaneous Drought Stress at Canopy Level Using Sun-Induced Chlorophyll Fluorescence and Canopy Reflectance, Remote Sensing, 14, 2642, https://doi.org/10.3390/rs14112642, 2022.

Delpierre, N., Berveiller, D., Granda, E., and Dufrêne, E.: Wood phenology, not carbon input, controls the interannual variability of wood growth in a temperate oak forest, New Phytologist, 210, 459–470, https://doi.org/10.1111/nph.13771, 2016.

Durand, M., Murchie, E. H., Lindfors, A. V., Urban, O., Aphalo, P. J., and Robson, T. M.: Diffuse solar radiation and canopy photosynthesis in a changing environment, Agricultural and Forest Meteorology, 311, 108684, https://doi.org/10.1016/j.agrformet.2021.108684, 2021.

https://doi.org/10.5194/egusphere-2024-657
Preprint. Discussion started: 19 March 2024

Frankenberg, C., Fisher, J. B., Worden, J., Badgley, G., Saatchi, S. S., Lee, J.-E., Toon, G. C., Butz, A., Jung, M., Kuze, A., and Yokota, T.: New global observations of the terrestrial carbon cycle from GOSAT: Patterns of plant fluorescence with gross primary productivity: CHLOROPHYLL FLUORESCENCE FROM SPACE, Geophysical Research Letters, 38, n/a-n/a, https://doi.org/10.1029/2011GL048738, 2011.

Gamon, J. A., Peñuelas, J., and Field, C. B.: A narrow-waveband spectral index that tracks diurnal changes in photosynthetic efficiency, Remote Sensing of Environment, 41, 35–44, https://doi.org/10.1016/0034-4257(92)90059-S, 1992.

Goulas, Y., Fournier, A., Daumard, F., Champagne, S., Ounis, A., Marloie, O., and Moya, I.: Gross Primary Production of a Wheat Canopy Relates Stronger to Far Red Than to Red Solar-Induced Chlorophyll Fluorescence, Remote Sensing, 9, 97, https://doi.org/10.3390/rs9010097, 2017.

Helm, L. T., Shi, H., Lerdau, M. T., and Yang, X.: Solar-induced chlorophyll fluorescence and short-term photosynthetic response to drought, Ecological Applications, 30, https://doi.org/10.1002/eap.2101, 2020.

Hmimina, G., Dufrêne, E., and Soudani, K.: Relationship between photochemical reflectance index and leaf ecophysiological and biochemical parameters under two different water statuses: towards a rapid and efficient correction method using real-time measurements: Disentangling PRI variability, Plant Cell Environ, 37, 473–487, https://doi.org/10.1111/pce.12171, 2014.

Hu, M., Cheng, X., Zhang, J., Huang, H., Zhou, Y., Wang, X., Pan, Q., and Guan, C.: Temporal Variation in Tower-Based Solar-Induced Chlorophyll Fluorescence and Its Environmental Response in a Chinese Cork Oak Plantation, Remote Sensing, 15, 3568, https://doi.org/10.3390/rs15143568, 2023.

Intergovernmental Panel On Climate Change: Climate Change and Land: IPCC Special Report on Climate Change, Desertification, Land Degradation, Sustainable Land Management, Food Security, and Greenhouse Gas Fluxes in Terrestrial Ecosystems, 1st ed., Cambridge University Press, https://doi.org/10.1017/9781009157988, 2022.

Jonard, F., De Cannière, S., Brüggemann, N., Gentine, P., Short Gianotti, D. J., Lobet, G., Miralles, D. G., Montzka, C., Pagán, B. R., Rascher, U., and Vereecken, H.: Value of sun-induced chlorophyll fluorescence for quantifying hydrological states and fluxes: Current status and challenges, Agricultural and Forest Meteorology, 291, 108088, https://doi.org/10.1016/j.agrformet.2020.108088, 2020.

Kim, J., Ryu, Y., Dechant, B., Lee, H., Kim, H. S., Kornfeld, A., and Berry, J. A.: Solar-induced chlorophyll fluorescence is non-linearly related to canopy photosynthesis in a temperate evergreen needleleaf forest during the fall transition, Remote Sensing of Environment, 258, 112362, https://doi.org/10.1016/j.rse.2021.112362, 2021.

Kováč, D., Ač, A., Šigut, L., Peñuelas, J., Grace, J., and Urban, O.: Combining NDVI, PRI and the quantum yield of solar-induced fluorescence improves estimations of carbon fluxes in deciduous and evergreen forests, Science of The Total Environment, 829, 154681, https://doi.org/10.1016/j.scitotenv.2022.154681, 2022.

Li, Y.-T., Gao, H.-Y., and Zhang, Z.-S.: Effects of Environmental and Non-Environmental Factors on Dynamic Photosynthetic Carbon Assimilation in Leaves under Changing Light, Plants, 12, 2015, https://doi.org/10.3390/plants12102015, 2023.

Lu, X., Liu, Z., Zhao, F., and Tang, J.: Comparison of total emitted solar-induced chlorophyll fluorescence (SIF) and top-of-canopy (TOC) SIF in estimating photosynthesis, Remote Sensing of Environment, 251, 112083, https://doi.org/10.1016/j.rse.2020.112083, 2020.

Magney, T. S., Barnes, M. L., and Yang, X.: On the Covariation of Chlorophyll Fluorescence and Photosynthesis Across Scales, Geophysical Research Letters, 47, https://doi.org/10.1029/2020GL091098, 2020.

Marrs, J. K., Reblin, J. S., Logan, B. A., Allen, D. W., Reinmann, A. B., Bombard, D. M., Tabachnik, D., and Hutyra, L. R.: Solar-Induced Fluorescence Does Not Track Photosynthetic Carbon Assimilation Following Induced Stomatal Closure, Geophysical Research Letters, 47, https://doi.org/e2020GL087956 10.1029/2020gl087956, 2020.

https://doi.org/10.5194/egusphere-2024-657
Preprint. Discussion started: 19 March 2024

Martini, D., Sakowska, K., Wohlfahrt, G., Pacheco-Labrador, J., van der Tol, C., Porcar-Castell, A., Magney, T. S., Carrara, A., Colombo, R., El-Madany, T. S., Gonzalez-Cascon, R., Martín, M. P., Julitta, T., Moreno, G., Rascher, U., Reichstein, M., Rossini, M., and Migliavacca, M.: Heatwave breaks down the linearity between sun-induced fluorescence and gross primary production, New Phytologist, 233, 2415–2428, https://doi.org/10.1111/nph.17920, 2022.

Maysonnave, J., Delpierre, N., François, C., Jourdan, M., Cornut, I., Bazot, S., Vincent, G., Morfin, A., and Berveiller, D.: Contribution of deep soil layers to the transpiration of a temperate deciduous forest: quantification and implications for the modelling of productivity, Ecology, https://doi.org/10.1101/2022.02.14.480025, 2022.

Miao, G., Guan, K., Suyker, A. E., Yang, X., Arkebauer, T. J., Walter-Shea, E. A., Kimm, H., Hmimina, G. Y., Gamon, J. A., Franz, T. E., Frankenberg, C., Berry, J. A., and Wu, G.: Varying Contributions of Drivers to the Relationship Between Canopy Photosynthesis and Far-Red Sun-Induced Fluorescence for Two Maize Sites at Different Temporal Scales, Journal of Geophysical Research: Biogeosciences, 125, https://doi.org/10.1029/2019JG005051, 2020.

Mohammed, G. H., Colombo, R., Middleton, E. M., Rascher, U., van der Tol, C., Nedbal, L., Goulas, Y., Pérez-Priego, O., Damm, A., Meroni, M., Joiner, J., Cogliati, S., Verhoef, W., Malenovský, Z., Gastellu-Etchegorry, J.-P., Miller, J. R., Guanter, L., Moreno, J., Moya, I., Berry, J. A., Frankenberg, C., and Zarco-Tejada, P. J.: Remote sensing of solar-induced chlorophyll fluorescence (SIF) in vegetation: 50 years of progress, Remote Sensing of Environment, 231, 111177, https://doi.org/10.1016/j.rse.2019.04.030, 2019.

Monteith, J. L.: Solar radiation and productivity in tropical ecosystems, Journal of Applied Ecology, 9, 747–766, 1972.

Moya, I., Loayza, H., López, M. L., Quiroz, R., Ounis, A., and Goulas, Y.: Canopy chlorophyll fluorescence applied to stress detection using an easy-to-build micro-lidar, Photosynthesis Research, 142, 1–15, https://doi.org/10.1007/s11120-019-00642-9, 2019.

Pierrat, Z., Magney, T., Parazoo, N. C., Grossmann, K., Bowling, D. R., Seibt, U., Johnson, B., Helgason, W., Barr, A., Bortnik, J., Norton, A., Maguire, A., Frankenberg, C., and Stutz, J.: Diurnal and Seasonal Dynamics of Solar-Induced Chlorophyll Fluorescence, Vegetation Indices, and Gross Primary Productivity in the Boreal Forest, Journal of Geophysical Research: Biogeosciences, 127, e2021JG006588, https://doi.org/10.1029/2021JG006588, 2022a.

Pierrat, Z. A., Bortnik, J., Johnson, B., Barr, A., Magney, T., Bowling, D. R., Parazoo, N., Frankenberg, C., Seibt, U., and Stutz, J.: Forests for forests: combining vegetation indices with solar-induced chlorophyll fluorescence in random forest models improves gross primary productivity prediction in the boreal forest, Environ. Res. Lett., 17, 125006, https://doi.org/10.1088/1748-9326/aca5a0, 2022b.

Porcar-Castell, A., Tyystjärvi, E., Atherton, J., van der Tol, C., Flexas, J., Pfündel, E. E., Moreno, J., Frankenberg, C., and Berry, J. A.: Linking chlorophyll a fluorescence to photosynthesis for remote sensing applications: mechanisms and challenges, Journal of Experimental Botany, 65, 4065–4095, https://doi.org/10.1093/jxb/eru191, 2014.

Soudani, K., Hmimina, G., Dufrêne, E., Berveiller, D., Delpierre, N., Ourcival, J.-M., Rambal, S., and Joffre, R.: Relationships between photochemical reflectance index and light-use efficiency in deciduous and evergreen broadleaf forests, Remote Sensing of Environment, 144, 73–84, https://doi.org/10.1016/j.rse.2014.01.017, 2014.

Soudani, K., Delpierre, N., Berveiller, D., Hmimina, G., Pontailler, J.-Y., Seureau, L., Vincent, G., and Dufrêne, É.: A survey of proximal methods for monitoring leaf phenology in temperate deciduous forests, Biogeosciences, 18, 3391–3408, https://doi.org/10.5194/bg-18-3391-2021, 2021.

Sukhova, E., Yudina, L., Kior, A., Kior, D., Popova, A., Zolin, Y., Gromova, E., and Sukhov, V.: Modified Photochemical Reflectance Indices as New Tool for Revealing Influence of Drought and Heat on Pea and Wheat Plants, Plants, 11, 1308, https://doi.org/10.3390/plants11101308, 2022.

Sun, Y., Gu, L., Wen, J., van der Tol, C., Porcar-Castell, A., Joiner, J., Chang, C. Y., Magney, T., Wang, L., Hu, L., Rascher, U., Zarco-Tejada, P., Barrett, C. B., Lai, J., Han, J., and Luo, Z.: From remotely sensed solar-

https://doi.org/10.5194/egusphere-2024-657
Preprint. Discussion started: 19 March 2024

induced chlorophyll fluorescence to ecosystem structure, function, and service: Part I—Harnessing theory, Global Change Biology, 29, 2926–2952, https://doi.org/10.1111/gcb.16634, 2023a.

Sun, Y., Wen, J., Gu, L., Joiner, J., Chang, C. Y., van der Tol, C., Porcar-Castell, A., Magney, T., Wang, L., Hu, L., Rascher, U., Zarco-Tejada, P., Barrett, C. B., Lai, J., Han, J., and Luo, Z.: From remotely-sensed solar-induced chlorophyll fluorescence to ecosystem structure, function, and service: Part II—Harnessing data, Global Change Biology, 29, 2893–2925, https://doi.org/10.1111/gcb.16646, 2023b.

Tucker, C. J.: Red and photographic infrared linear combinations for monitoring vegetation, Remote Sensing of Environment, 8, 127–150, https://doi.org/10.1016/0034-4257(79)90013-0, 1979.

Wang, N., Clevers, J. G. P. W., Wieneke, S., Bartholomeus, H., and Kooistra, L.: Potential of UAV-based sun-induced chlorophyll fluorescence to detect water stress in sugar beet, Agricultural and Forest Meteorology, 323, 109033, https://doi.org/10.1016/j.agrformet.2022.109033, 2022.

Wang, X., Chen, J. M., and Ju, W.: Photochemical reflectance index (PRI) can be used to improve the relationship between gross primary productivity (GPP) and sun-induced chlorophyll fluorescence (SIF), Remote Sensing of Environment, 246, 111888, https://doi.org/10.1016/j.rse.2020.111888, 2020.

Xiao, J., Chevallier, F., Gomez, C., Guanter, L., Hicke, J. A., Huete, A. R., Ichii, K., Ni, W., Pang, Y., Rahman, A. F., Sun, G., Yuan, W., Zhang, L., and Zhang, X.: Remote sensing of the terrestrial carbon cycle: A review of advances over 50 years, Remote Sensing of Environment, 233, 111383, https://doi.org/10.1016/j.rse.2019.111383, 2019.

Xiao, J., Fisher, J. B., Hashimoto, H., Ichii, K., and Parazoo, N. C.: Emerging satellite observations for diurnal cycling of ecosystem processes, Nat. Plants, 7, 877–887, https://doi.org/10.1038/s41477-021-00952-8, 2021.

Xu, S., Atherton, J., Riikonen, A., Zhang, C., Oivukkamäki, J., MacArthur, A., Honkavaara, E., Hakala, T., Koivumäki, N., Liu, Z., and Porcar-Castell, A.: Structural and photosynthetic dynamics mediate the response of SIF to water stress in a potato crop, Remote Sensing of Environment, 263, 112555, https://doi.org/10.1016/j.rse.2021.112555, 2021.

Zanotelli, D., Asensio, D., Schwarz, M., Benyahia, F., Hammerle, A., Abdelkader, A. B., Campos, F. B., Callesen, T., Andreotti, C., Montagnani, L., Tagliavini, M., and Wohlfahrt, G.: Vineyard water and carbon dioxide exchange during a heat wave, Copernicus Meetings, https://doi.org/10.5194/egusphere-egu23-10124, 2023.

Zeng, Y., Hao, D., Huete, A., Dechant, B., Berry, J., Chen, J. M., Joiner, J., Frankenberg, C., Bond-Lamberty, B., Ryu, Y., Xiao, J., Asrar, G. R., and Chen, M.: Optical vegetation indices for monitoring terrestrial ecosystems globally, Nat Rev Earth Environ, 3, 477–493, https://doi.org/10.1038/s43017-022-00298-5, 2022.

Zhang, J., Xiao, J., Tong, X., Zhang, J., Meng, P., Li, J., Liu, P., and Yu, P.: NIRv and SIF better estimate phenology than NDVI and EVI: Effects of spring and autumn phenology on ecosystem production of planted forests, Agricultural and Forest Meteorology, 315, 108819, https://doi.org/10.1016/j.agrformet.2022.108819, 2022.

Zhang, Z., Chen, J. M., Zhang, Y., and Li, M.: Improving the ability of solar-induced chlorophyll fluorescence to track gross primary production through differentiating sunlit and shaded leaves, Agricultural and Forest Meteorology, 341, 109658, https://doi.org/10.1016/j.agrformet.2023.109658, 2023.